Molecular Plant
Research Article

CellPress
Partner Journal

The miR319-Targeted GhTCP4 Promotes the Transition from Cell Elongation to Wall Thickening in Cotton Fiber

Jun-Feng Cao[1,2,3,8], Bo Zhao[1,3,8], Chao-Chen Huang[1,3,4,8], Zhi-Wen Chen[1], Ting Zhao[5], Hong-Ru Liu[1], Guan-Jing Hu[6], Xiao-Xia Shangguan[1], Chun-Min Shan[1,3], Ling-Jian Wang[1], Tian-Zhen Zhang[5], Jonathan F. Wendel[6], Xue-Ying Guan[5,*] and Xiao-Ya Chen[1,3,4,7,*]

[1]National Key Laboratory of Plant Molecular Genetics, Institute of Plant Physiology and Ecology/CAS Center for Excellence in Molecular Plant Sciences, Chinese Academy of Sciences, Shanghai 200032, China

[2]Plant Stress Biology Center, Institute of Plant Physiology and Ecology/CAS Center for Excellence in Molecular Plant Sciences, Chinese Academy of Sciences, Shanghai 200032, China

[3]University of Chinese Academy of Sciences, Shanghai 200032, China

[4]School of Life Science and Technology, ShanghaiTech University, Shanghai 201210, China

[5]Agronomy Department, College of Agriculture and Biotechnology, Zhejiang University, Hangzhou, Zhejiang 310058, China

[6]Department of Ecology, Evolution and Organismal Biology, Iowa State University, Ames, IA 50011, USA

[7]Plant Science Research Center, Shanghai Key Laboratory of Plant Functional Genomics and Resources, Shanghai Chenshan Botanical Garden, Shanghai 201602, China

[8]These authors contributed equally to this article.

***Correspondence: Xue-Ying Guan (xueyingguan@zju.edu.cn), Xiao-Ya Chen (xychen@sibs.ac.cn)**

https://doi.org/10.1016/j.molp.2020.05.006

ABSTRACT

Plant cell growth involves a complex interplay among cell-wall expansion, biosynthesis, and, in specific tissues, secondary cell wall (SCW) deposition, yet the coordination of these processes remains elusive. Cotton fiber cells are developmentally synchronous, highly elongated, and contain nearly pure cellulose when mature. Here, we report that the transcription factor GhTCP4 plays an important role in balancing cotton fiber cell elongation and wall synthesis. During fiber development the expression of miR319 declines while GhTCP4 transcript levels increase, with high levels of the latter promoting SCW deposition. GhTCP4 interacts with a homeobox-containing factor, GhHOX3, and repressing its transcriptional activity. GhTCP4 and GhHOX3 function antagonistically to regulate cell elongation, thereby establishing temporal control of fiber cell transition to the SCW stage. We found that overexpression of *GhTCP4A* upregulated and accelerated activation of the SCW biosynthetic pathway in fiber cells, as revealed by transcriptome and promoter activity analyses, resulting in shorter fibers with varied lengths and thicker walls. In contrast, *GhTCP4* downregulation led to slightly longer fibers and thinner cell walls. The GhHOX3–GhTCP4 complex may represent a general mechanism of cellular development in plants since both are conserved factors in many species, thus providing us a potential molecular tool for the design of fiber traits.

Key words: cell elongation, secondary cell wall, cotton fiber, *Gossypium hirsutum*, TCP, microRNA

Cao J.-F., Zhao B., Huang C.-C., Chen Z.-W., Zhao T., Liu H.-R., Hu G.-J., Shangguan X.-X., Shan C.-M., Wang L.-J., Zhang T.-Z., Wendel J.F., Guan X.-Y., and Chen X.-Y. (2020). The miR319-Targeted GhTCP4 Promotes the Transition from Cell Elongation to Wall Thickening in Cotton Fiber. Mol. Plant. **13**, 1063–1077.

INTRODUCTION

Cotton fibers, the natural material widely used in textile industry, are single-celled trichomes that develop from initials on the seed epidermis and successively undergo rapid elongation and secondary cell wall (SCW) biosynthesis. When mature, cotton fibers are composed of nearly pure (>95%) cellulose (Applequist et al., 2001; Kim and Triplett, 2001; Lee et al., 2007; Mansoor and

Published by the Molecular Plant Shanghai Editorial Office in association with Cell Press, an imprint of Elsevier Inc., on behalf of CSPB and IPPE, CAS.

This is an open access article under the CC BY-NC-ND license (http://creativecommons.org/licenses/by-nc-nd/4.0/).

Paterson, 2012). Plant cell growth is associated with dynamic processes of cell-wall biosynthesis, loosening, and expansion (Cosgrove, 2005; Kang et al., 2019). Osmoregulation of primary cell-wall extension has been proposed to drive cotton fiber elongation, which gradually terminates with the onset of SCW deposition (Ruan et al., 2001; Qin and Zhu, 2011; Hu et al., 2019). Due to their large size (sometimes >4 cm in length) and developmental synchrony, cotton fibers provide a unique model for investigation of plant cell growth and wall formation.

In *Arabidopsis thaliana* the MYB–bHLH–WD40 (MBW) complex controls the initiation of leaf and stem trichomes; the R2R3 MYB transcription factor GLABRA1 (GL1) plays a key role in activation of the expression of *GLABRA2* (*GL2*), encoding a member of the homeodomain leucine zipper (HD-ZIP) IV transcription factor subfamily, which in turn regulates trichome cell growth (Szymanski et al., 2000). In cotton fiber cells. homologs of the MBW complex are all expressed (Lee et al., 2007; Shangguan et al., 2008); however, genetic analyses indicated that it is the MIXTA-type R2R3 MYB factors that determine cotton fiber initiation (Walford et al., 2011; Paterson et al., 2012; Tan et al., 2016; Wu et al., 2018). Despite this difference, a homolog of *Arabidopsis* GL2, GhHOX3, also regulates cotton fiber cell elongation, and its activity is modulated by the growth hormone gibberellin through interaction with the DELLA protein (Shan et al., 2014).

SCW deposition strengthens plant organs but restricts cell growth (Cosgrove, 2005; Xu et al., 2014; Huang et al., 2018; Kang et al., 2019). Length and strength are the two key parameters of cotton fiber quality, the latter being closely related to cell-wall properties. Observations with transmission electron microscopy (TEM) have revealed an inverse relationship between cotton fiber length and wall thickness: the diploid cotton species *Gossypium arboreum* produces short fibers with a thicker wall, whereas cultivars of the extra-long staple cotton *Gossypium barbadense* and the widely cultivated upland cotton *Gossypium hirsutum* have long and fine lint (Hernandez-Gomez et al., 2015).

Cellulose, the structural component of both primary and secondary cell walls, is a polysaccharide consisting of linear β-1,4-glucan chains synthesized by the cellulose synthase complex (Bashline et al., 2014; McFarlane et al., 2014; Takenaka et al., 2018). Plants have evolved a set of enzymes that synthesize the SCW, and the NAC–MYB–CESAs module defines a central pathway of SCW cellulose biosynthesis, in which the NAC (NAM, ATAF1,2, and CUC2) transcription factors act as the primary switch (Taylor-Teeples et al., 2015). In *G. hirsutum* the NAC factor GhFSN1 has been shown to regulate SCW biosynthesis in fiber, and its overexpression with the 35S promoter increases wall thickness and mildly reduces fiber length (Zhang et al., 2018), implying a tradeoff between cell elongation and SCW deposition. Two independent studies showed that the cotton MYB transcription factor genes expressed in fiber cells could induce transcription of the SCW CESA genes when introduced into *A. thaliana* (Sun et al., 2015; Huang et al., 2016). Additionally, dual functions in cotton fiber elongation and SCW formation have been linked to a conserved LIM-domain-containing protein, WLIM1a, which is, however, not responsible for cellulose biosynthesis (Han et al., 2013). Although duration of the elongation stage is among the most important factors that determine cotton fiber length (Dai et al., 2017), to date the molecular mechanism underlying the termination of cell elongation and the activation of SCW synthesis remains obscure.

The TCP (TEOSINTE BRANCHED1/CYCLOIDEA/PROLIFERATING CELL FACTOR1) transcription factors constitute a plant-specific family and contain a conserved non-canonical basic helix-loop-helix (bHLH) domain responsible for DNA binding and protein–protein interactions (Kosugi and Ohashi, 1997; Nath et al., 2003; Palatnik et al., 2003). TCPs can be separated into two major groups, classes I and II, the latter being further divided into two types, CYC/TB1 (ECE) and CINCINNATA (CIN). In *Arabidopsis* there are 11 class II TCP genes, of which five CIN types (*TCP2*, *TCP3*, *TCP4*, *TCP10*, and *TCP24*) are targeted by miR319 (Kosugi and Ohashi, 1997; Nath et al., 2003; Palatnik et al., 2003) and function in diverse aspects of plant growth and development. For example, *Arabidopsis* TCP4 is involved in cell proliferation, trichome development, leaf morphogenesis, plant maturation, and senescence (Nath et al., 2003; Palatnik et al., 2003; Efroni et al., 2008; Schommer et al., 2008; Vadde et al., 2018), and promotes hypocotyl elongation through integrating environmental and hormonal signals (Challa et al., 2016) but reduces the stature of the mature plant when overexpressed (Palatnik et al., 2003). Furthermore, TCP4 was shown to regulate SCW biosynthesis in xylem vessel elements through activation of the NAC gene *VDN7* (Sun et al., 2017). In cotton, functions of several TCP genes have been reported. The class I TCP factor GhTCP14 of *G. hirsutum* was shown to activate auxin signaling to mediate epidermal cell differentiation and elongation (Wang et al., 2013). Another class I TCP, GbTCP of *G. barbadense*, affects fiber elongation through a complex interplay involving jasmonic acid biosynthesis and ethylene signaling (Hao et al., 2012). GhTCP13 and two other class II TCPs are functionally redundant in modulating plant architecture (Diao et al., 2019).

Here, we show that in cotton GhTCP4, a CIN-type TCP transcription factor regulated by miR319, interacts with GhHOX3 to coordinate fiber cell elongation and SCW biosynthesis, two events that are key to cotton fiber traits. During fiber development, the temporal expression pattern of GhTCP4 is important in controlling the transition to and the pace of SCW deposition.

RESULTS

GhTCP4 is Associated with Cotton Fiber Formation

Our previous studies have identified two regulators of cotton fiber elongation, the homeobox-containing transcription factor GhHOX3 and the atypical bHLH factor GhPRE1, of which GhHOX3 plays a pivotal role (Shan et al., 2014; Zhao et al., 2018). With GhHOX3 as bait, yeast two-hybrid (Y2H) screening of a *G. hirsutum* fiber cDNA library identified ten interacting candidates, including a TCP protein (Shan et al., 2014) which, based on phylogenetic analysis, is a close homolog of *A. thaliana* TCP4 (AtTCP4) belonging to the class II CIN-type TCPs (Supplemental Figure 1). Accordingly, we named it GhTCP4. It has a typical TCP domain located in the N terminus (Supplemental Figure 2).

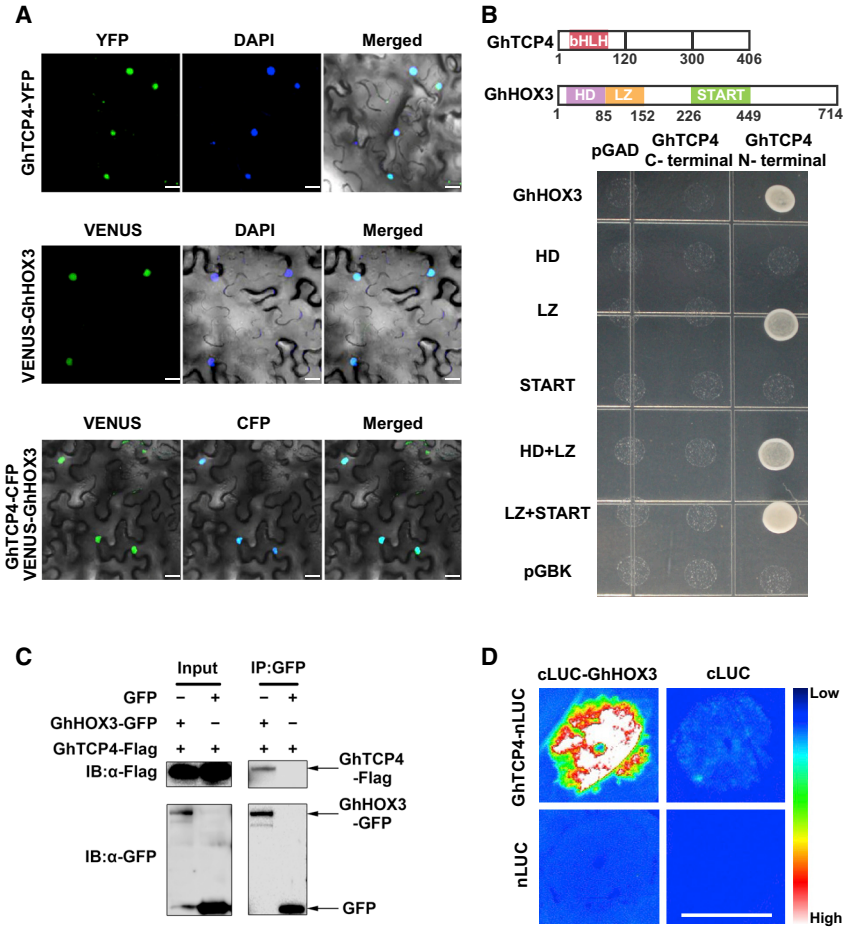

Figure 1. GhTCP4 Interacts with GhHOX3.

(A) Subcellular localization assays of GhTCP4A and GhHOX3, showing nuclear localization of GhTCP4-YFP (upper) and VENUS-GhHOX3 (middle) and co-localization of GhTCP4-CFP and VENUS-GhHOX3 in the nucleus (bottom). *Agrobacterium* cells harboring the fusion protein genes were infiltrated into leaves of *Nicotiana benthamiana* through the abaxial surface, and 72 h later the samples were observed under a confocal microscope (LSM510, Zeiss). Scale bar, 10 μm.

(B) Yeast two-hybrid assay of GhTCP4A-GhHOX3 interaction. Domains (above) and their positions (below) are indicated. The GhTCP4 N-terminal fragment of 120 amino acids showed binding to the leucine-zipper (LZ) domain of GhHOX3. Yeast was grown on SD/-Leu/-Trp/-His medium supplemented with 10 mM 3-amino-1,2,4-triazole.

(C) Detection of GhTCP4A-GhHOX3 interaction by co-immunoprecipitation. GhTCP4-FLAG, GhHOX3-GFP, and GFP were expressed in pairs in *N. benthamiana* leaf cells; crude proteins were immunoprecipitated with anti-GFP antibody beads and detected with anti-FLAG antibody. Total proteins (input) and proteins after immunoprecipitation (IP) were detected by anti-FLAG antibody (above) and anti-GFP antibody (below). The GhTCP4-FLAG and GFP pair served as a control, in which the GhTCP4-FLAG protein was undetectable. GhTCP4-FLAG was detected in the GhTCP4-FLAG and GhHOX3-GFP co-expression sample. IB, immunoblot.

(D) BiFC assay. GhHOX3 and GhTCP4A were fused to the C- and N-terminal ends of the LUC reporter (cLUC and nLUC) to form GhHOX3-cLUC and GhTCP4-nLUC, and truncated LUC and the chimeric genes were co-expressed in *N. benthamiana* leaves in pairs as indicated. The nLUC and cLUC vectors, nLUC and cLUC-GhHOX3, and cLUC and GhTCP4-nLUC were co-expressed as negative controls. Fluorescence intensities indicate the strength of protein–protein binding. Scale bar, 1 cm.

In tobacco (*Nicotiana benthamiana*) leaves, the GhTCP4A-CFP and VENUS-GhHOX3 fusion proteins co-localized in the nucleus (Figure 1A). We then divided GhTCP4A into two fragments and tested their interactions with GhHOX3 in yeast; we found that the bHLH-embedded N-terminal fragment of GhTCP4 is responsible for binding to the leucine zipper (LZ) domain of GhHOX3 (Figure 1B). Hence, we performed *in vivo* co-immunoprecipitation (coIP). GhTCP4-FLAG and GhHOX3-GFP were transiently co-expressed in tobacco leaves; after precipitation of the leaf proteins with anti-GFP antibody beads, the GhTCP4-FLAG fusion protein was readily detected (Figure 1C). In a bimolecular fluorescence complementation (BiFC) assay, the split luciferase proteins (nLUC and cLUC) fused with GhTCP4A and GhHOX3, respectively, also showed strong interaction in tobacco leaves, whereas the empty vectors (nLUC and cLUC) or the empty vector with one of the partners (nLUC with cLUC-GhHOX3 and cLUC with GhTCP4-nLUC) did not (Figure 1D). In addition to GhTCP4, GhHOX3 also interacted with other CIN-type TCPs in yeast (Supplemental Figure 3). The interaction with GhHOX3 hinted at a role of GhTCP4 in cotton fiber development.

In the cotton genus (*Gossypium*), four species were independently domesticated and are cultivated for spinnable fiber: the A-genome diploids *Gossypium herbaceum* and *G. arboreum*, and the AD-genome allotetraploids *G. hirsutum* and *G. barbadense* (Wendel and Grover, 2015; Chen et al., 2020; Huang et al., 2020). The *G. hirsutum* genome harbors 72 putative TCP genes (Hu et al., 2019), of which 15 belong to the class II CIN type with eight in subgenome A and seven in subgenome D (Supplemental Tables 1 and 2). *GhTCP4A* (GH_A04G0407) and *GhTCP4D* (GH_D05G3657) are located on chromosomes A04 and D05, respectively (Supplemental Figure 4), and both encode proteins of 401 amino acids (aa) that share 97% sequence identity (Supplemental Figure 2).

Analysis by quantitative real-time PCR (qRT–PCR) showed that *GhTCP4* was expressed in various tissues of *G. hirsutum* (Figure 2A), and in transcriptome data transcripts of the two homoeologous genes were present at a similar level (Supplemental Figure 5). In fiber cells, the *GhTCP4* transcript level was low at the fiber-initiation stage, became increasingly elevated following fiber elongation, peaked during the transition from rapid elongation to the SCW synthesis stages (9–12 days post anthesis [DPA]), then remained relatively high but declined progressively (Figure 2B). Compared with the fiber elongation gene *GhHOX3*, which reached its peak expression 3 days earlier (6 DPA) and dropped sharply afterward (Supplemental

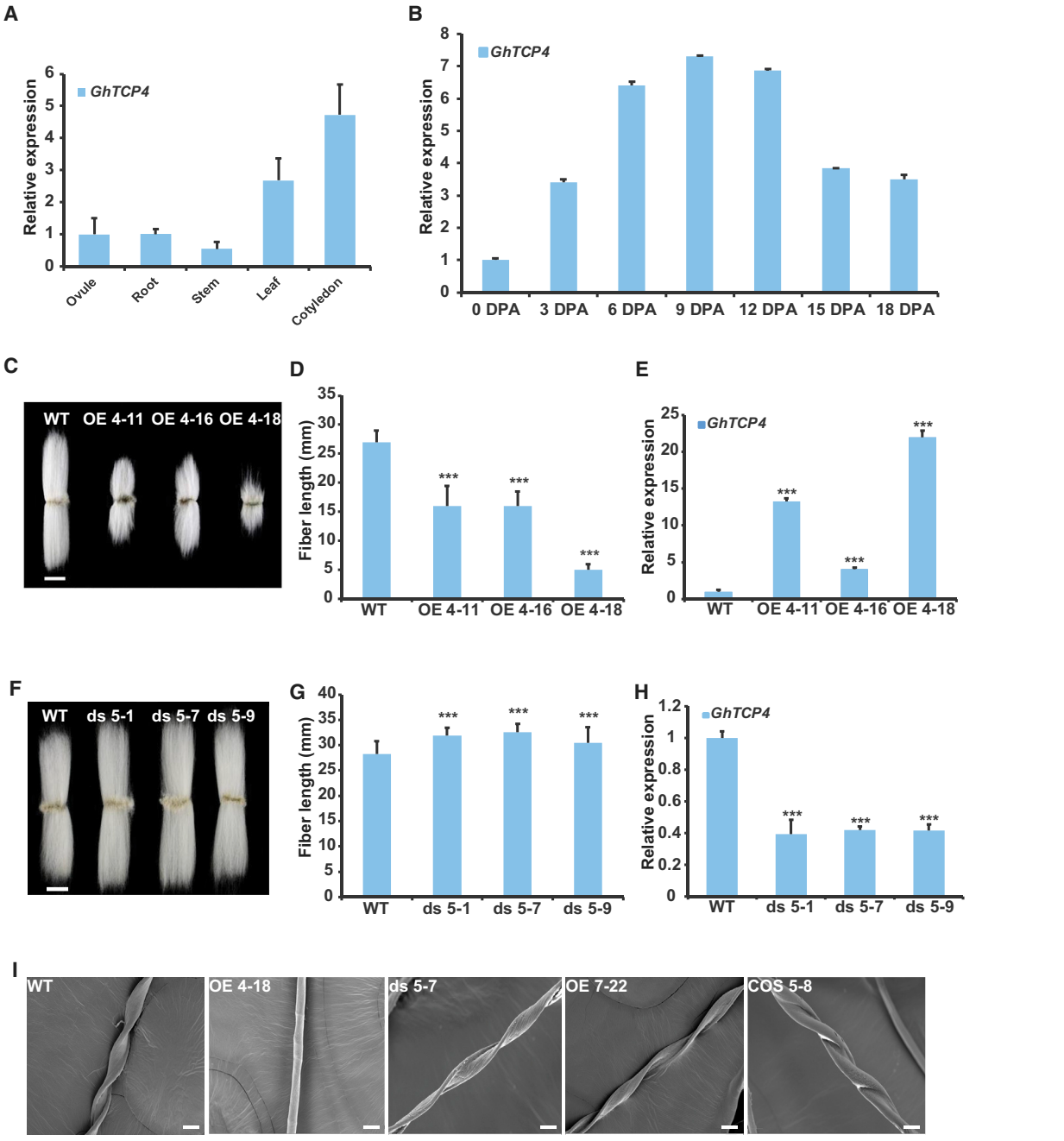

Figure 2. GhTCP4 Negatively Regulates Fiber Length and Affects Fiber Twisting.

(A and B) Relative expression of *GhTCP4* in different organs of *G. hirsutum* **(A)** and in ovules (0 DPA) and developing fiber cells on the day post anthesis (DPA) as indicated **(B)**. qRT–PCR was performed using *GhHIS3* (AF024716) as an internal reference, and expression in 0-DPA ovules was set to 1 (means of triplicates ± SD).

(C–E) Analysis of mature fiber from *pRDL1*::*mGhTCP4A* overexpression (OE) cotton lines, with wild-type (WT) *G. hirsutum* cv. R15 as the control. **(C)** Image of fibers from the transgenic T2 lines. Scale bar, 1 cm. **(D)** Fiber length (mean ± SD, $n = 30$, $^{***}P < 0.001$, Student's *t*-test). **(E)** Relative expression of *GhTCP4* in 9-DPA fiber cells; expression in WT was set to 1 (means of triplicates ± SD).

(F–H) Analysis of mature fibers of *p35S*::*dsGhTCP4* (ds) lines. **(F)** Image of fibers from the RNAi (ds) lines, T2. Scale bar, 1 cm. **(G)** Fiber length (mean ± SD, $n = 30$, $^{***}P < 0.001$, Student's *t*-test). **(H)** Relative expression of *GhTCP4* in 9-DPA fiber cells; expression in WT was set to 1 (means of triplicates ± SD).

(I) Scanning electron microscopy (SEM) view of mature fibers. While the mature fibers of the WT, *GhTCP4* silencing (ds5–7), *GhmiR319a* overexpression (OE miR319), and GhHOX3 co-suppression (COS 5–8) lines were twisted, the *GhTCP4* overexpression line (OE4–18) fiber appeared stick-like without twisting. Scale bar, 10 μm.

Figure 5), *GhTCP4* exhibited a flatter and temporally delayed expression pattern during fiber development (Figure 2B).

In transient expression assays with tobacco leaf cells the GhTCP4A-YFP fusion protein localized to the nucleus (Figure 1A), consistent with its function as a transcription factor. Searching cotton quantitative trait locus (QTL) information (Lacape et al., 2010), we found that *GhTCP4* was associated with QTLs fiber length, micronaire, and uniformity (Supplemental Figure 4), implying that GhTCP4 is possibly involved in fiber elongation and synchronous growth.

GhTCP4 Overexpression Represses Cotton Fiber Elongation

Sequence analysis showed that, like *AtTCP4*, a putative miR319-binding site is present in the open reading frame (ORF) of *GhTCP4* and of other CIN-type TCP genes of *G. hirsutum* (Supplemental Figure 6A). To provide experimental evidence that miR319 cleaves the mRNA of *GhTCP4*, we overexpressed *MIR319* (*GhmiR319a*) with the 35S promoter and the miR319-resistant form of *GhTCP4A* (*mGhTCP4A*) with the fiber-preferential *GhRDL1* promoter in *G. hirsutum*. We then performed 5′-rapid amplification of cDNA ends (5′RACE) on the cotton fiber RNAs. Gel analysis showed that, compared with wild type (WT), more full-length *GhTCP4* cDNAs of the expected size could be amplified from the *mGhTCP4A* line harboring the miR319-binding site mutation than from the *p35S*::*GhMIR319* sample, in which the full-length band was below the detectable level (Supplemental Figure 6B). Further degradome sequencing revealed that the cleavage site was located at nucleotide 968 in *GhTCP4A* (Supplemental Figure 6C). Cleavage of other CIN-type *GhTCP* gene transcripts by miR319 was also detected (Supplemental Figure 6D).

The *pRDL1*::*mGhTCP4A* cotton plants produced strikingly shorter fibers with uneven lengths among fiber cells (Figure 2C–2E), as well as less-serrated leaves and bracts (Supplemental Figure 7A). In contrast, downregulation by RNAi (*p35S*::*dsGhTCP4*) led to slightly longer fibers (Figure 2F–2H and Supplemental Table 3) and deeper-serrated leaves and bracts (Supplemental Figures 7 and 8), resembling the leaf phenotype of the miR319-overexpression mutant *jaw-D* of *A. thaliana* (Palatnik et al., 2003). Thus, *GhTCP4* overexpression reduced fiber length, and the expression level had to be controlled properly to sustain cotton fiber cell growth. Testing of the fiber quality indicated that the micronaire was also affected in the *dsGhTCP4* lines (Supplemental Table 3). Consistent with this, under scanning electron microscopy (SEM), the fiber texture appeared different among the WT and the transgenic lines (Figure 2I), which will be discussed later. Together, these data support the notion that GhTCP4 is associated with fiber parameters such as length and micronaire (Supplemental Figure 4B).

The Expression Patterns of *MIR319* Genes in Cotton Fiber

A limited examination of the genomes of flowering plants revealed possible expansion of the *MIR319* gene family in the Malvaceae, especially in cotton species. There are seven genes annotated as encoding *MIR319* precursors in the diploid A- and D-genome species *G. arboreum* and *Gossypium raimondii*, respectively, and the copy numbers are doubled in the allotetraploid species *G. hirsutum* and *G. barbadense* (Figure 3A and Supplemental Table 4). *Theobroma cacao*, a Malvaceae species distantly related to cotton, has six *MIR319* genes, compared to three in *A. thaliana*, two in *Oryza sativa*, and nine in the hexaploid wheat *Triticum aestivum*. Analysis by qRT–PCR showed that, contrary to *GhTCP4*, whose expression increased during fiber elongation and early SCW synthesis stages (Figure 2B), *MIR319* genes were highly expressed in the ovules at 0 DPA and in the fiber cells during early elongation (to 3 DPA), thereafter decreasing in expression (Figure 3B and Supplemental Figure 9A–9F). The *MIR319* and *TCP4* genes also exhibited opposite expression dynamics in *G. arboreum* fiber cells (Figure 3C and Supplemental Figure 9G).

GhTCP4 is just one of the TCP family genes in cotton that harbor the miR319-binding site. In *G. hirsutum* overexpressing *GhmiR319a* (*p35S*::*GhMIR319*), other putative target genes, including *GhTCP2*, *GhTCP3*, and *GhTCP10*, were also downregulated (Figure 3D), consistent with the finding from analysis of degradome data that their transcripts could be cleaved at the miR319 recognition site (Supplemental Figure 6). Nevertheless, the TCP expression dynamics may vary depending on growth conditions, and other factors, particularly transcriptional regulation, also play an important role. Notably, similar to the *dsGhTCP4* lines, the surviving *p35S*::*GhMIR319* cotton plants developed longer fibers (Figure 3E–3G).

GhTCP4 Interacts with GhHOX3 and Represses Its Transcriptional Activity

Among the *pRDL1*::*mGhTCP4A* plants, the high-expression line OE4-18 produced fuzzy-like short fibers, with the length reduced by more than 70% compared with the WT fibers (Figure 4A), reminiscent of the fiber elongation defect caused by silencing of *GhHOX3*, a key regulator of cotton fiber elongation (Shan et al., 2014). *GhRDL1* and *GhEXPA1* are the direct targets of GhHOX3 and encode cell-wall-loosening proteins (Xu et al., 2013; Shan et al., 2014). We found that both genes were downregulated in the *GhTCP4*-OE fiber cells (Figure 4B and 4C) as in the *GhHOX3*-suppression line COS5-8 (Shan et al., 2014), despite *GhHOX3* expression not being repressed (Figure 4D). These data suggest functional antagonism between the two transcription factors.

Considering the protein–protein interaction results (Figure 1), we asked whether binding to GhTCP4A would affect GhHOX3 activity as a transcription factor. We used the *GhRDL1* and *GhEXPA1* promoters to drive expression of the luciferase (LUC) reporter (Figure 4E), which was clearly activated by GhHOX3 in tobacco leaf cells (Figure 4F and 4G), as previously reported (Shan et al., 2014). However, when GhTCP4A was co-expressed with GhHOX3, the LUC activity dropped drastically (Figure 4E and 4F). GhHD1, another HD-ZIP IV factor of cotton, was previously found to associate with GhHOX3 (Shan et al., 2014); the activity of this transcriptional complex was also decreased by GhTCP4A (Figure 4H and 4I). Thus, GhTCP4 acts as a repressor of GhHOX3 in controlling the expression of cell-wall-expansion genes.

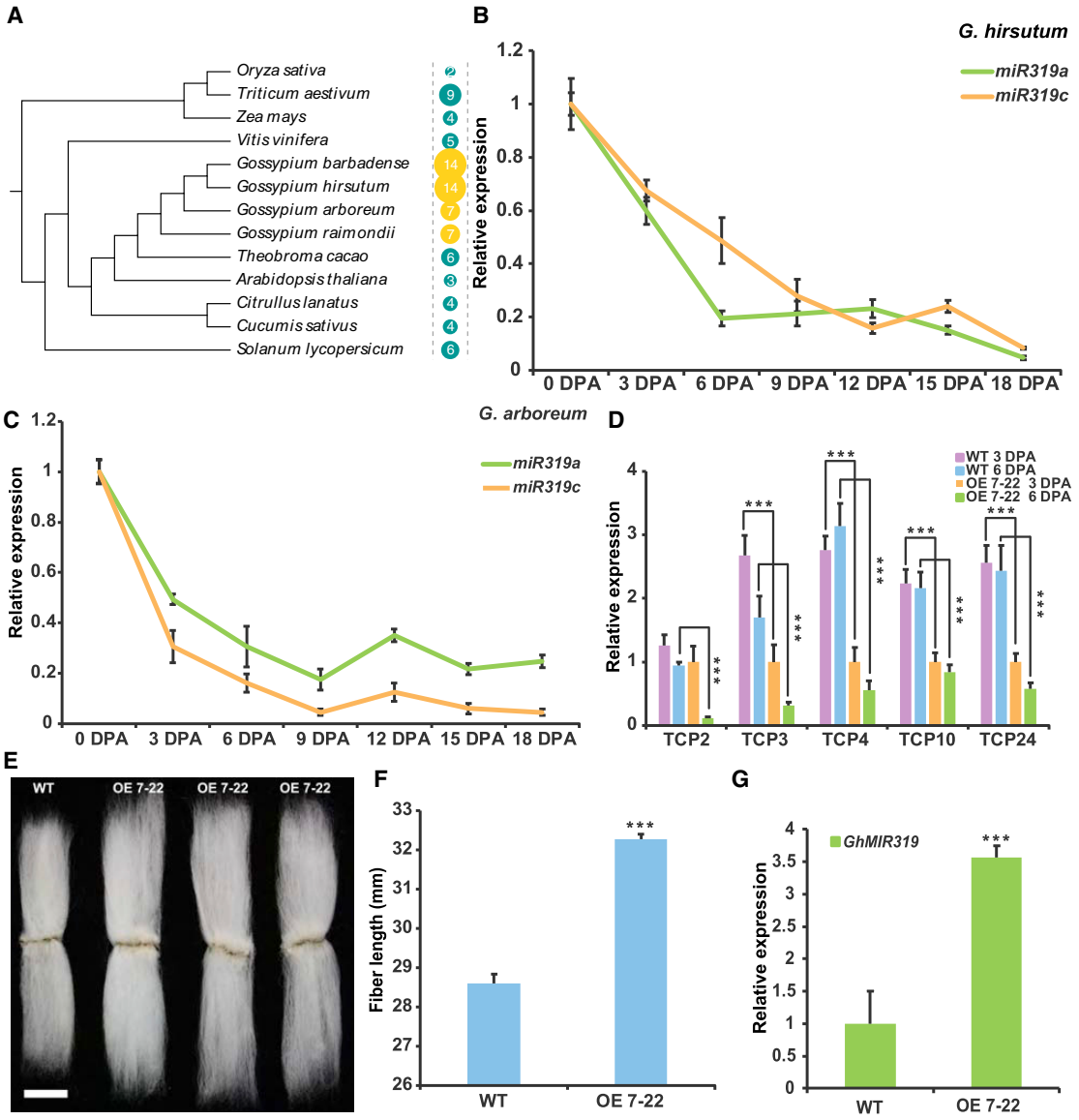

Figure 3. The miR319-GhTCP4 Module Regulates Cotton Fiber Growth and Development.

(A) Copy numbers of *MIR319* genes in 10 dicotyledon and three monocotyledon species. The phylogenetic tree was constructed by Time Tree (www.timetree.org).

(B and C) Relative expression of mature miR319 in 0-DPA ovules and developing fiber cells of *G. hirsutum* **(B)** and *G. arboreum* **(C)** as indicated; the level in the 0-DPA sample was set to 1 (means of triplicates ± SD). U6 served as an internal reference.

(D) Relative expression the miR319-targeted *GhTCP* genes in fiber cells of WT *G. hirsutum* and a miR319-overexpression line (OE 7–22); expression in the 3-DPA fiber of OE miR319 was set to one (means of triplicates ± SD, ***$P < 0.001$, Student's *t*-test).

(E and F) View of mature fiber **(E)** and fiber length **(F)** of WT *G. hirsutum* and the miR319-overexpression line (OE 7–22) (mean ± SD, $n = 30$, ***$P < 0.001$, Student's *t*-test). T2. Scale bar, 1 cm.

(G) The relative level of miR319 in the WT (set to 1) and transgenic (OE 7–22) fiber cells (means of triplicates ± SD, ***$P < 0.001$, Student's *t*-test), at 6 DPA.

To analyze the functional consequences of GhHOX3–GhTCP4 interaction in cotton, we crossed the *GhHOX3*-silencing (*dsHOX3*) line with the *GhTCP4*-overexpression (OE4-18) and -silencing (ds5-7) lines. We found that the cotton fibers remained short in the *dsHOX3* background regardless of the changes in *GhTCP4* expression (Supplemental Figure 10), suggesting that the two factors may act in the same pathway, at least partly, to modulate fiber elongation. However, as a transcription factor, GhTCP4 may have an additional function in fiber cell extensibility.

GhTCP4 Expedites Cell-Wall Thickening

To analyze the effects of GhTCP4 on cotton fiber texture, we first observed the fibers of WT and transgenic lines under SEM. The fuzz-like fiber of the *GhHOX3*-silencing line COS5-8 showed the clear twisting characteristic of the WT fiber (Figure 2I). However, for the *GhTCP4*-overexpression line OE4-18 the twisting disappeared and the fiber cells appeared stick-like. By contrast, the *dsGhTCP4* (ds5-7) fiber cells appeared thinner (Figure 2I). Examination of the mature fiber under TEM showed that, in

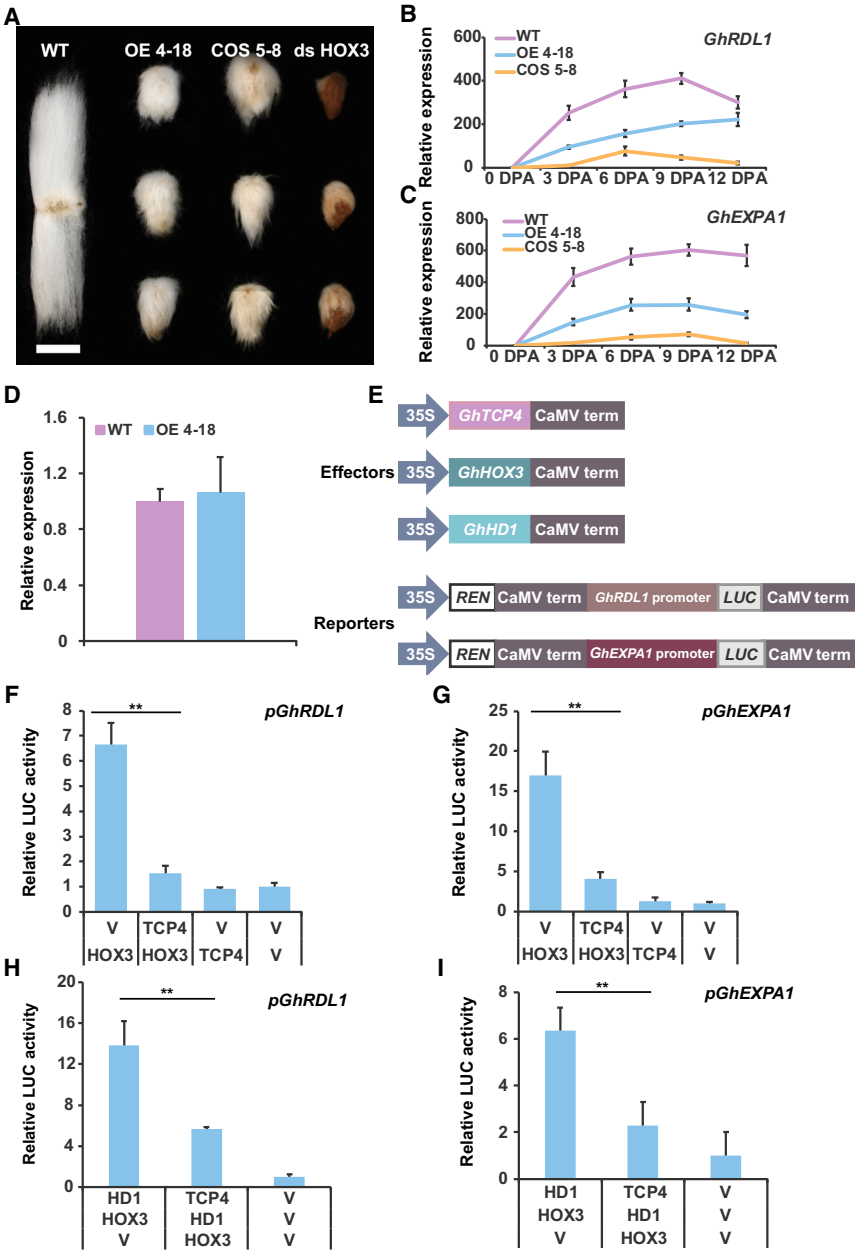

Figure 4. GhTCP4 Represses the Function of GhHOX3.

(A) Fiber at maturation stage from the *pRDL1*::*mGhTCP4A* overexpression line (OE4–18, T7 generation) and *GhHOX3*-suppression lines (COS5-8, dsHOX3, T9 generation). Scale bar, 1 cm.

(B and C) Relative expression of cell-wall-loosening genes *GhRDL1* **(B)** and *GhEXPA1* **(C)** in fiber cells; expression in WT 0-DPA ovules was set to 1 (means of triplicates ± SD).

(D) Relative expression of *GhHOX3* in fiber cells of the WT and *GhTCP4* OE4–18 line of *G. hirsutum*. Expression in WT 6-DPA fiber cells was set to 1 (means of triplicates ± SD).

(E) Schematic map of promoter-luciferase reporters and effectors.

(F–I) Effects of GhTCP4A on activation of the promoters of *pGhRDL1* and *pGhEXPA1* by GhHOX3 **(F and G)** and by GhHOX3+GhHD1 **(H and I)**. The LUC and effector constructs **(E)** were introduced into *N. benthamiana* leaves; V represents an equal volume of bacteria harboring empty vector. The relative LUC activities were normalized to the reference Renilla (REN) luciferase. The activities relative to empty vector (set to 1) are shown, mean ± SD, $n = 4$, $^{**}P < 0.01$, Student's *t*-test.

cross-section, the *GhTCP4*-OE fiber was nearly solid without a lumen because of the much thicker cell wall, whereas the *dsGhTCP4* fiber had a significantly thinner cell wall than the WT control (Supplemental Figure 11A–11C). These data suggest an important role of GhTCP4 in regulation of SCW formation.

We then used TEM to observe the cell wall at different stages of cotton fiber development (Figure 5). During rapid elongation (9 DPA) there was little change in cell-wall thickness (Supplemental Figure 11D). At the SCW synthesis stage (18 DPA), the thickness of the *GhTCP4*-OE fiber wall was doubled in comparison with that of the WT, and in contrast the fiber cell walls of the *dsGhTCP4* lines were thinner (Figure 5A and 5D). This difference in fiber cell-wall thickness was elaborated during the later SCW stage (21 DPA; Figure 5B and 5E) and at the onset of maturation (27 DPA; Figure 5C and 5F). The thinnest fiber cell walls were found in the miR319-overexpression line (Figure 5A–5F), in which not only *GhTCP4* but other putative target *TCPs* were downregulated (Figure 3D). In addition, the OE4-18 fibers exhibited a smaller diameter, implying limited cell expansion in that growth plane (Figure 5A–5C). These data indicate that *GhTCP4* overexpression accelerated SCW deposition and increased cell-wall thickness.

GhTCP4 Promotes Cellulose Biosynthesis at SCW Synthesis Stages

To gain further insights into the biological function of GhTCP4, we sampled 6- and 12-DPA fiber cells from the WT, *GhTCP4*-overexpression (OE4-18), and *GhTCP4*-downregulation (ds5-7) cotton plants for RNA sequencing. Principal component analysis of the transcriptomes showed that the ds5-7 and WT fibers were close to each other at 6 DPA, the elongation stage, after which they became clearly separated during the transition to the SCW stage (12 DPA), implying that GhTCP4 functions more in the later stage. However, the OE4-18 fiber samples at the two stages were not only strikingly different from their WT counterparts but also well separated from each other (Supplemental Figure 12A and 12B). Indeed, while there was a relatively small number (154) of differentially expressed genes (DEGs) present in the dsTCP4 (ds5-7) fiber compared with the WT fiber at 6 DPA, there were many more DEGs (~5000) in the OE4-18 fiber.

Analysis of the DEGs detected in the 12-DPA OE4-18 fibers revealed that carbohydrate metabolism and cell-wall biogenesis

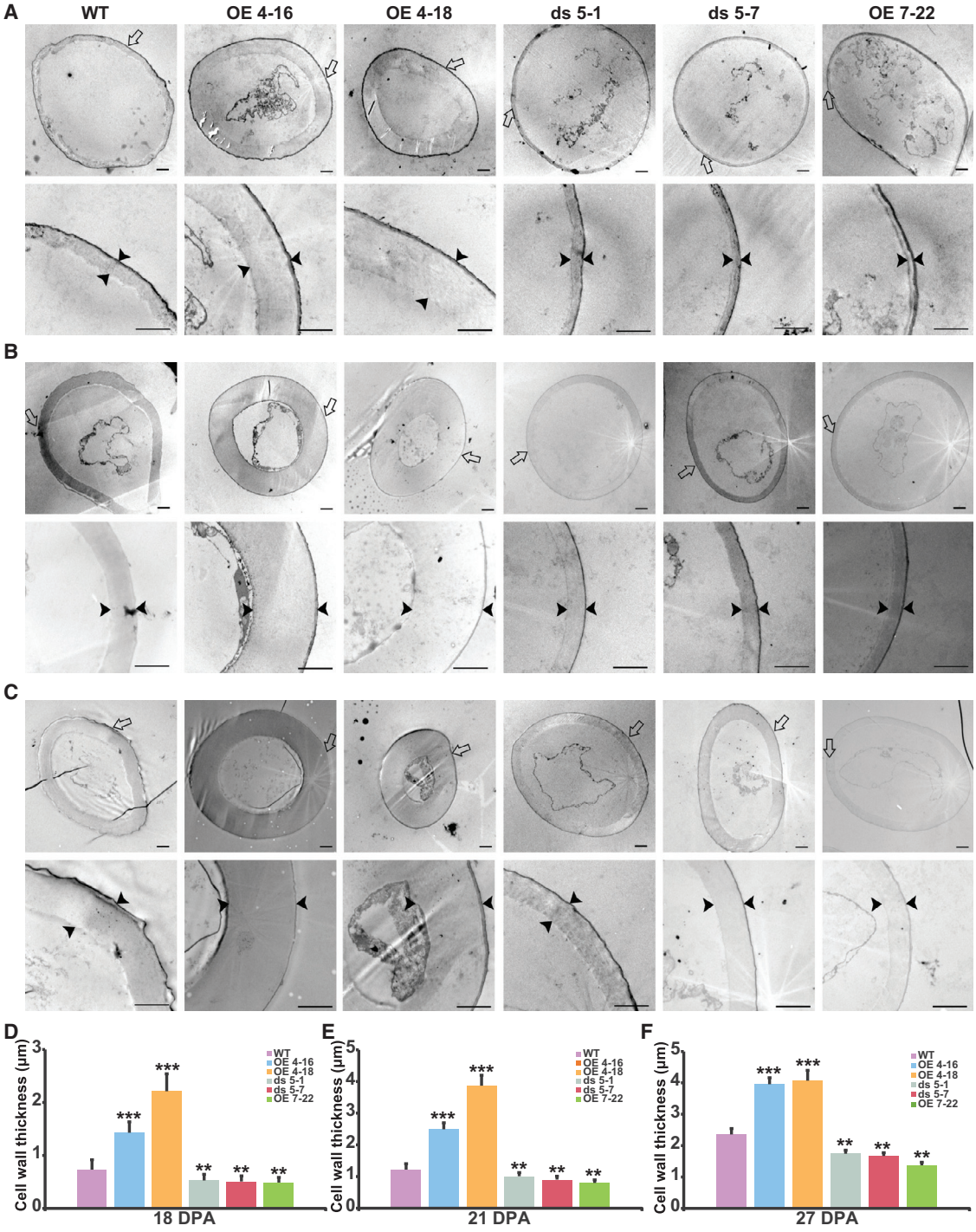

Figure 5. GhTCP4 Promotes Cell-Wall Thickening.

(A–C) TEM view of cross-sections of cotton fiber cells (upper) and cell walls (bottom) of the WT, *GhTCP4* overexpression (OE4–16, OE4–18), *GhTCP4* RNAi (ds5-1, ds5-7), and *GhmiR319a* overexpression (OE7–22) lines of *G. hirsutum*, sampled at 18 **(A)**, 21 **(B)**, and 27 **(C)** DPA. Scale bar, 2 μm. The bottom panels are magnified images of regions (indicated with hollow arrows) of the fibers in the upper panels. The cell walls are marked by solid arrows. Scale bars, 2 μm.

(D–F) Fiber cell-wall thickness of the cotton lines as indicated (mean ± SD, $n = 100$, $^{**}P < 0.01$, $^{***}P < 0.001$, Student's *t*-test).

were among the highly enriched functional categories (Supplemental Figure 12C). The NAC–MYB signaling cascade has been shown to regulate the expression of CESA genes (Huang et al., 2015). Remarkably, 22 of the CESA genes, as well as 27 NAC and 76 MYB transcription factor genes, were upregulated in the overexpression line or downregulated in the silencing line at 12 DPA (Supplemental Tables 5–8). The CESAs responsible for cotton fiber primary cell wall (PCW) and SCW

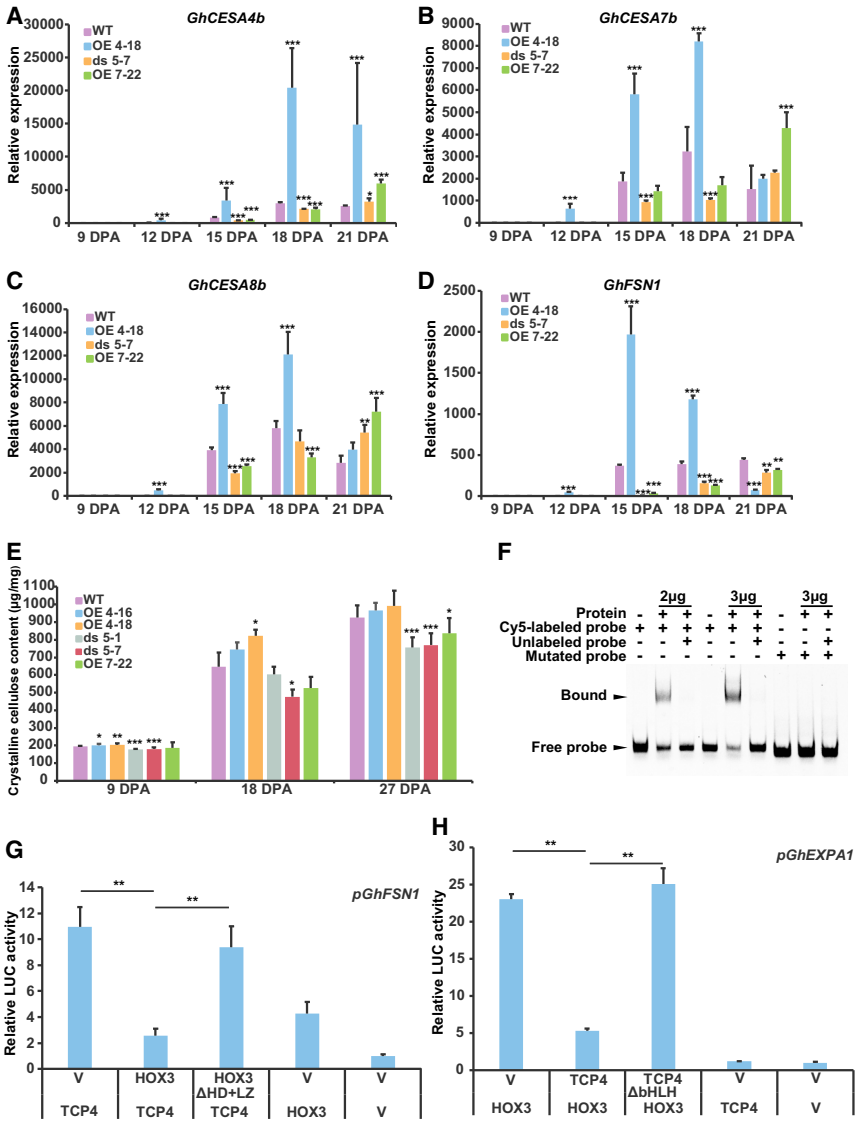

Figure 6. GhTCP4 Activates SCW Cellulose Biosynthetic Genes.

(A–D) Relative expression levels of SCW biosynthesis genes in fiber cells of WT, *GhTCP4*-overexpression (OE4–18), and *GhTCP4* RNAi (ds5-7), and *MIR319* overexpression (OE7–22) *G. hirsutum* lines, determined by qRT–PCR. Expression in WT 9-DPA fibers was set to 1 (means of triplicates ± SD, $^{**}P < 0.01$, $^{***}P < 0.001$, Student's *t*-test). *GhFSN1* and the three *GhCESA* genes were highly upregulated in OE4–18 and downregulated in ds5-7 lines during the SCW stage (12–18 DPA). The *CESA* genes analyzed are *GhCESA4b* (Gh_A08G0421, Gh_D08G0509), *GhCESA7b* (Gh_A05G3965, Gh_D05G0079), and *GhCESA8b* (Gh_A10G0327, Gh_D10G0333). See also Supplemental Figure 14.

(E) Crystalline cellulose contents in fiber cells at different stages as indicated (μg cellulose/mg alcohol-insoluble residues; $n = 4$, mean ± SD, $^{*}P < 0.05$, $^{**}P < 0.01$, $^{***}P < 0.001$ compared with WT, Student's *t*-test).

(F) Electrophoretic mobility shift assay of the *pGhFSN1* promoter. The promoter fragment (~70 bp, harboring the TCP4-binding TGGGCC motif) was labeled with cy5, and the double-stranded DNA fragments (5 ng) were incubated with the GhTCP4A protein (2 μg). Excess unlabeled fragments (100-times cy5-fragments) were added to compete for the binding site. As a negative control, a mutated probe (TGGGCC deletion) was similarly labeled and assayed. Incubation of the *pGhFSN1* fragment with 2 μg of GhTCP4A protein resulted in a shifted band; this shift was reduced by adding the unlabeled probe, enhanced by increasing the protein amount to 3 μg, and abolished when the TGGGCC motif in the labeled probe was deleted (mutated probe).

(G and H) The reciprocal effects of GhHOX3 and GhTCP4A. Promoters of *pGhFSN1* (~2k, **G**) and *pGhEXPA1* (~2k, **H**) were fused to the LUC reporter and infiltrated into tobacco leaves together with the effector(s) as indicated. For truncated versions, GhHOX3ΔHD-LZ (without 25–152 aa) and GhTCP4ΔbHLH (without 25–110 aa) were amplified from the CDSs by overlapping PCR. The LUC activities were normalized to REN, and values relative to the empty vector control (set to 1) are shown. V represents one volume of bacteria with empty vector (mean ± SD, $n = 4$, $^{**}P < 0.01$, Student's *t*-test).

biosynthesis have been classified on the basis of their temporal expression patterns and homology in BLAST searches; *GhCESA4*, *GhCESA7*, and *GhCESA8* are grouped together with *Arabidopsis CESA4*, *CESA7*, and *CESA8*, which are responsible for SCW, whereas *GhCESA1*, *GhCESA3*, and *GhCESA6* are homologous to PCW CESA genes of *Arabidopsis* (Yuan et al., 2015; Zhang et al., 2015). We then checked all CESAs identified in the RNA-sequencing data. We found that at the elongation stage (6 DPA), there was no significant difference in the expression of the CESA genes between the WT and the *GhTCP4*-OE line, which was confirmed by qRT–PCR (Supplemental Figure 13 and Supplemental Table 5), suggesting that GhTCP4 had less impact on cellulose synthesis in the PCW. In contrast, for CESA genes preferentially expressed at the SCW stage after 12 DPA, their transcript levels were drastically elevated in the overexpression line (Supplemental Table 6). Further qRT–PCR analysis of *GhCESA4*, *GhCESA7*, *GhCESA8*, and the NAC gene *GhFSN1* demonstrated that not only were these genes upregulated in *GhTCP4*-OE fibers but also that they were expressed earlier (Figure 6A–6D and Supplemental Figure 14).

The changes in expression of SCW CESA genes prompted us to compare cellulose deposition in the transgenic and WT fiber cells. We found that at 18 DPA (SCW synthesis stage) the crystalline cellulose in the total alcohol-insoluble residue (AIR) of fiber was 10%–20% higher in the *GhTCP4-OE* lines than in the WT (Figure 6E). At the maturation stage (27 DPA), cellulose made up over 95% of the AIR in both WT and *GhTCP4*-OE fibers, but in *GhTCP4*-silencing fibers it was ~80% of the AIR (Figure 6E), implying deaccelerated SCW biosynthesis in the fibers with downregulated *GhTCP4*. Quantitative analysis by gas chromatography–mass spectrometry (GC–MS) revealed that, at 18 DPA, the *GhTCP4*-OE fiber contained lower amounts of

non-cellulosic monosaccharides than the WT control; in contrast, the levels were strikingly high in the *dsGhTCP4* fiber (Supplemental Figure 15). These data strongly support the notion that *GhTCP4* regulates SCW formation and the pace of fiber development.

TCP transcription factors can bind to the GGNCC or GGNNCC *cis* elements (Kosugi and Ohashi, 2002), and class II TCPs such as OsTB1 and AtTCP4 were reported to specifically recognize TGGGC(C/T) (González-Grandío and Cubas, 2016), which is present in the promoter regions of *GhFSN1* and *GhCESA7* (Supplemental Table 9). An electrophoretic mobility shift assay (EMSA) using the *GhFSN1* and *GhCESA7* promoter fragments showed that GhTCP4A indeed bound to the promoters of these genes (Figure 6F and Supplemental Figure 16), and the binding reaction was an endothermic process, as determined by an isothermal titration calorimetry (ITC) assay (Supplemental Figure 16C). We then selected other candidate genes for an extended EMSA analysis; these genes are SCW biosynthesis-related, upregulated in the *GhTCP4*-OE fibers, and contain the TCP recognition motif in their promoters. GhTCP4 exhibited binding to 12 promoters out of the 14 genes assayed, including those encoding glucan endo-1,3-β-glucosidase and peroxidase (Supplemental Figure 17).

Lastly, as GhHOX3 can bind to the GhTCP4A N-terminal fragment harboring the DNA-binding domain (Figure 1B), we asked whether this interaction would affect the transcriptional activation of target genes by GhTCP4. In a dual-luciferase assay using *N. benthamiana* leaf cells, GhTCP4A clearly activated the *GhFSN1* promoter, but activation was significantly attenuated by GhHOX3 (Figure 6G). When the N-terminal fragment harboring the LZ domain, which is involved in GhTCP4 binding (Figure 1B), was deleted, the inhibition was diminished (Figure 6G). Similar results were obtained when the *GhCESA7* promoter was assayed (Supplemental Figure 16B). Reciprocally, GhTCP4 also repressed the transcriptional activity of GhHOX3 toward its target genes *GhEXPA1* and *GhRDL1*, and the N-terminal fragment involved in protein–protein interaction was also required for repression (Figure 6H and Supplemental Figure 18).

In summary, GhTCP4 can recognize the *cis* element in promoters of *GhFSN1* and *GhCESA7* to activate gene expression, and GhHOX3 interferes with this activity. We anticipate that GhTCP4 promotes SCW deposition by directly regulating a set of SCW genes, including the key transcription factor *GhFSN1*. The temporal expression patterns of the miR319-targeted TCP genes, including *GhTCP4*, play an important role in determining the duration and rates of fiber elongation and SCW synthesis.

DISCUSSION

Over the past decade a great deal has been learned about the complex biology of cotton fiber development (Mansoor and Paterson, 2012; Paterson et al., 2012; Guan et al., 2014). The emerging view is that elongation is characterized by multiple interacting physiological pathways, including hormone signaling, cell-wall-loosening and -extension processes, and lipid metabolism (Ruan et al., 2001; Qin et al., 2007; Xu et al., 2013; Shan et al., 2014; Hu et al., 2016; Zhang et al., 2017), whereas the SCW stage is dominated by cellulose synthesis (Gou et al., 2007; Lee et al., 2007; Tuttle et al., 2015). This extraordinary dynamism in the temporal development of a single cell is incompletely understood, but insights into some of the key triggers are beginning to emerge.

Data from genetic, biochemical, and molecular analyses demonstrated that GhHOX3 and GhTCP4 are the key regulators of the two stages of fiber development and that they coordinate these stages by directly interacting with each other. The relative changes in their expression levels during fiber development affect the physiological status in the fiber cell. Additional components of this regulatory system include the phytohormone gibberellin, which promotes fiber elongation through degradation of the DELLA protein that binds to GhHOX3 (Shan et al., 2014), and miR319, which controls expression of the class II CIN-type TCP genes including *GhTCP4*. Our interpretation, which is modeled in Figure 7, is that the GhHOX3–GhTCP4 complex functions as a switch in transducing the developmental signals from cell elongation to cell-wall thickening. We noticed that downregulation of *GhTCP4* delayed cell-wall biosynthesis (Figures 5 and 6) and increased fiber length (Figure 2). Both evolutionary and genetic studies of cotton species have linked a higher growth rate and prolonged growth stage to superior spinnable fiber formation (Applequist et al., 2001; Kim and Triplett, 2001; Lee et al., 2007; Mansoor and Paterson, 2012; Fang et al., 2017; Wang et al., 2017; Du et al., 2018; Ma et al., 2018). It thus seems plausible that *MIR319*, the target *TCP* genes, and other components of this regulatory module can potentially be used for improving fiber traits through genome editing to modify the timing and amount of expression.

Previous studies showed that loss of function of CIN-type TCPs led to a prolonged cell division stage and abnormal leaf shape in *Arabidopsis* and *Antirrhinum* (Nath et al., 2003; Palatnik et al., 2003), and that overexpression of miR319 in *Arabidopsis* resulted in immature morphology of leaf cells (Efroni et al., 2008); thus, the miR319-TCP module plays a role in developmental timing. Distinct from multicellular leaf tissues, the extensively elongated cotton fiber is single celled and does not undergo cell division after initiation; however, the miR319–TCP4 module still acts as a regulator of cellular phase transition. The interaction between the CIN-type TCPs and the cell elongation factor GhHOX3 generates a temporal pattern that synchronizes elongation and wall thickening among individual fiber cells. Indeed, *GhTCP4* overlaps with fiber uniformity QTL regions. Thus, miR319–TCP4 is involved in generation of heterochrony in multicellular tissues and synchrony in specialized groups of single cells.

The HD-ZIP-IV and CIN-type TCP transcription factors are both conserved in land plants (Rombola-Caldentey et al., 2014; Sun et al., 2017), and the regulation of the transition from cell elongation to SCW biosynthesis by the HOX–TCP pair may not be confined to cotton fiber. In *Arabidopsis* the miR319-regulated TCPs also function in SCW biosynthesis in xylem (Sun et al., 2017) and, notably, both cotton fiber and primary xylem vessel elements are highly elongated cells that synthesize SCWs. Another feature shared by the two groups of transcription factors is that they function in concert with members of the same family or other types of regulators

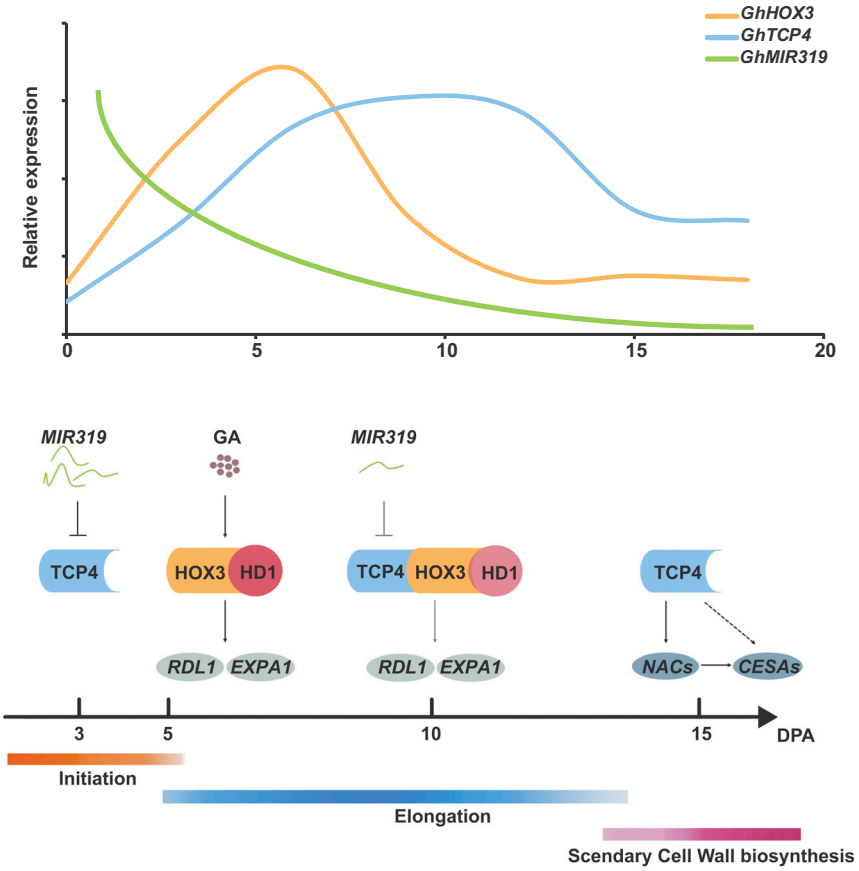

Figure 7. A Proposed Model Decipting How Cotton Fiber Development Is Regulated by the miR319-GhTCP4 Module.

After fiber initiation, the GhHOX3 level increases rapidly and the phytohormone gibberellin (GA) promotes fiber cell elongation at least partly through GhHOX3. Meanwhile, the miR319 level declines and levels of its target GhTCP4 and probably other target TCPs progressively increase; the TCPs inhibit GhHOX3 activity and promote SCW biosynthesis.

(Danisman et al., 2012; Rombola-Caldentey et al., 2014; Shan et al., 2014), and TCP4 may function differently depending on tissue type with respect to cell elongation, as in *Arabidopsis* seedlings where AtTCP4 promotes hypocotyl elongation (Challa et al., 2016). In addition to transcriptional regulation, a recently identified receptor-like kinase from *Arabidopsis*, AtVRLK1, negatively regulates SCW biosynthesis, implying the existence of a signaling pathway involved in SCW formation (Huang et al., 2018). Further identification of the factors that act together or sequentially with the GhHOX3–GhTCP4 complex will shed new light on the regulatory network that coordinates plant cell growth, wall expansion, and SCW deposition. These insights will likely facilitate genetic modification of cotton for desirable fiber traits and possibly many other species of plants for timber yield or quality.

METHODS

Plant Materials and Growth Conditions

Plants of *G. hirsutum* cv. R15, its transgenic lines, and *G. arboreum* cv. Qingyangxiaozi were grown in the greenhouse at 28°C ± 2°C under a 14-h light/10-h dark photoperiod, and in the field in Songjiang (Shanghai), Yuncheng (Shanxi Province), and Sanya (Hainan Province). For each line the mature fiber was harvested at random for measurements. At least 30 plants in each line were observed for phenotypic changes. The cotton bolls (fruits) were collected at the full-blossom stage (2–5 weeks after the first flower) from similar positions in each plant, and the developmental stage of each boll was recorded as DPA. For fiber quality, the samples (approximately 10 g for each sample) were tested by the Center of Cotton Fiber Quality Inspection and Testing, Chinese Ministry of Agriculture (Anyang, Henan Province, China). The leaves and bracts were collected at the same growth stage as indicated. Ovules (seeds) were harvested at the indicated DPA, and fibers were isolated by scratching the ovule with a metal strainer in liquid nitrogen. Plants of *N. benthamiana* and *A. thaliana* (Columbia-0) were grown at 28°C ± 2°C and 22°C ± 2°C, respectively, under a 16-h light/8-h dark photoperiod.

Plant Transformation and Crossing

The coding sequence of *GhTCP4A* (A denotes subgenome A) was PCR-amplified from a cDNA library of *G. hirsutum* cv. R15 with KOD FX Neo (TOYOBO, KFX-201), then inserted into the pCAMBIA 2301 vector behind the fiber-specific promoter *GhRDL1* (Wang et al., 2004; Shan et al., 2014). For RNAi, the sense and anti-sense *GhTCP4* fragments (~500 bp) harboring the *miR319*-binding site were amplified and separated by a 120-bp intron of *Arabidopsis RTM1*, and the fragment was cloned into pCAMBIA 2301 after the CaMV 35S promoter. Similarly, the *35S* promoter was used to overexpress the microRNA319 primary sequence (*MIR319a*, ~1.6k, Supplemental Table 9). For generating the miR319-resistant *mGhTCP4A*, the sequence of AGG GGA CCC CTT CAG TCC was changed to CGA GGC CCA TTG CAA AGC by overlapping PCR, and *mGhTCP4A* was placed behind the *GhRDL1* promoter. For *GhTCP4* overexpression (*RDL1*::*mGhTCP4*) and silencing (*35S*::*dsGhTCP4*), at least five independent transformants for each construct were generated, and three transgenic lines for each construct (with different expression levels of the transgene) were used for analysis as specifically indicated. Primers used are listed in Supplemental Table 10. Sequences of some of the genes investigated are given in Supplemental Table 9, and the *G. hirsutum TCP* genes are numbered as published (Zhang et al., 2015); these numbers match those of the *Arabidopsis* TCPs.

The floral-dip method was used for *Arabidopsis* transformation (Bent, 2006). Cotton transformation was conducted as reported by Shangguan et al. (2008). In brief, hypocotyl segments from 1-week old cotton seedlings were used as explants for *Agrobacterium tumefaciens* infection, and plantlets were regenerated from the induced and proliferated calluses. Transgenic T0 generation plants were screened by β-glucuronidase (GUS) staining and PCR amplification of the transgene.

Pollen from the *GhHOX3* RNAi line *dsHOX3* was transferred to the emasculated flowers of *GhTCP4* overexpression line OE4-18 and the *GhTCP4* RNAi line ds5-7. Fiber length was measured on more than 30 seeds collected randomly from each plant.

Gene Sequence Analysis

To identify TCP genes in *Gossypium*, we retrieved the protein sequences of *G. arboreum* (Du et al., 2018), *G. raimondii* (Paterson et al., 2012),

G. barbadense, and *G. hirsutum* (Hu et al., 2019) from the Cottongen database (https://www.cottongen.org/). *TCP* genes were identified with the hidden Markov model (hmm) profile of the TCP domain PF03634 via HMMER (http://hmmer.janelia.org/), and the genes were mapped onto the genome by their chromosomal positions using jcvi (https://github.com/tanghaibao/jcvi). To identify *MIR319* genes in plant species, 132 mature sequences of *miR319* were retrieved from miRbase (http://www.mirbase.org/). Mature sequences were searched against the genome reference to detect homologous loci using BLASTN (Altschul et al., 1997). The 500-bp flanking sequences for each homologous locus were then extracted to evaluate the secondary structure. Sequences with a stem-loop structure and with the mature microRNA in the arms were considered *MIR319* genes. The *miR319* target genes of cotton TCPs were predicted by the online tool (http://plantgrn.noble.org/psRNATarget/analysis) and referred to the website (http://structuralbiology.cau.edu.cn/PNRD/index.php). Degradome sequencing of 3-DPA cotton fiber RNAs from the *GhmiR319a* overexpression line (*p35S::GhMIR319*) was performed to detect the cleaved transcripts.

Nucleic Acid Isolation and Expression Analysis

Cotton total RNA was extracted using the RNAprep Pure Plant Kit (Tiangen Biotech, Beijing, China). The RNA (1 μg) was used as a template for cDNA synthesis with the RT primer Mix (Random 6mers and Oligo dT Primer mixed) and PrimerScript RT Enzyme Mix I (TaKaRa). After 10-fold dilution, the products were used as template for qRT–PCR with SYBR-Green PCR Mastermix (TaKaRa) monitored on a thermal cycler (Mastercycler RealPlex; Eppendorf, Shanghai, China). A cotton histone-3 gene (*GhHIS3*, AF024716) was used as the internal reference. Cotton microRNAs were isolated with the miRcute Plant miRNA Isolation Kit (Tiangen Biotech, Beijing, China), and the miRcute Plus miRNA First-Strand cDNA Kit and miRcute Plus miRNA qPCR Kit (Tiangen Biotech) were used to perform reverse transcription and qRT–PCR on the Bio Rad 185-5201 CFX CONNECTION, using U6 as the internal reference.

RNA sequencing was performed by Biomarker Technologies (Beijing, China) on the 6- and 12-DPA fiber samples collected from the cotton plants. In brief, the libraries were generated using NEBNext UltraTM RNA Library Prep Kit for Illumina (NEB, USA); clean reads were annotated by searching against the published *G. hirsutum* genome data (Hu et al., 2019) and categorized by the Eukaryotic Orthologous Groups of proteins database (KOG). Gene expression levels were normalized and calculated as reads per kilobase per million reads. Genes with an adjusted P-value < 0.05 were assigned as DEGs (false discovery rate $\leq$ 0.001, absolute value of $\log_2$ ratio ≥ 1). The degradome sequencing was conducted by Biomarker Technologies. The library was constructed as described by Addo-Quaye et al. (2009), and after sequencing the clean reads were mapped to the reference genome sequence (Hu et al., 2019). Rfam was used to annotate the non-coding RNAs, and the remaining unannotated reads were used to detect the microRNA cleavage sites using CleaveLand3.0.

5′RACE was performed with the SMARTer RACE 5′/3′ Kit (Clontech Laboratories) according to the manufacturer's protocol. In brief, the 5′-terminal adapter was added to the total RNAs (1 μg) extracted from the 3-DPA fibers of WT (R15), miR319 overexpression (OE), and *GhTCP4* OE lines of *G. hirsutum* for reverse transcription. The *GhTCP4* specific primer (Supplemental Table 10) was used to perform 5′RACE PCR, and the amplified product was analyzed on an agarose gel.

Cell-Wall Analysis

The 9-, 18-, and 27-DPA, and mature fibers (~50 DPA) were harvested from WT and transgenic lines of *G. hirsutum* cv. R15 as indicated above. Samples were ground into powder in liquid nitrogen and the AIR was prepared as described previously (Pettolino et al., 2012; Song et al., 2014). In brief, ~50 mg of powder was washed with each of 70% ethanol, 1:1 (v/v) mixture of chloroform and methanol, and acetone to obtain the AIR. The crystalline cellulose content and the monosaccharide compositions were measured as reported by Foster et al. (2010) with minor changes. In brief, 2 mg of AIR was hydrolyzed by trifluoroacetic acid at 121°C for 90 min, and the supernatant was dried by a freeze dryer and dissolved in 100 μl *N*-methyl-*N*-(trimethylsilyl) trifluoroacetamide (Sigma) and 50 μl of pyridine for derivatization at 65°C for 10 min. A GC–MS system equipped with an SP-2380 capillary column (Agilent 5975 inert MSD system) was used to quantify the non-cellulosic monosaccharides. The remaining residues were degraded with anthrone sulfuric acid (Foster et al., 2010) to determine the content of crystalline cellulose.

Microscopic Observation

For protein subcellular localization, the coding region of *GhTCP4A* was fused to *YFP* or *CFP* by PCR, and the chimeric gene *p35S*::*GhTCP4-YFP* in the pCAMBIA2301 vector was introduced into *Agrobacterium* cells, which were infiltrated with a syringe into the abaxial surface of *N. benthamiana* leaves for transient expression. Three days later, the infiltrated areas were observed under a confocal microscope (LSM510, Zeiss). For co-localization the *p35S*::*GhTCP4-CFP* and *p35S*::*YFP-GhHOX3* fusion genes were assayed together.

Fibers attached to ovules were fixed in 2.5% glutaraldehyde in PBS (0.1 M, pH 7.4). The fixed samples were embedded in resin and cut into 1-μm-thick sections and observed with a light microscope (Zeiss Axioplan2 imaging). For surface structures, the samples were dried to a critical point with a dryer (Balzers CPD 020), stuck onto a brass disc with double-sided adhesive silver tape, coated with gold/palladium by a sputter-coating unit (Balzers CSD 004), and observed under a scanning electron microscope (Amray, 1830 I). For TEM ultrathin sections were made on a Leica EM UC6 ultramicrotome. Sections were scoped at 80 kV with a Philips CM 12 transmission electron microscope.

Protein–Protein and Protein–DNA Interactions

For EMSA, the *GhTCP4* coding sequence was inserted into the PET-32a vector and the protein product was purified by GenScript (Nanjing, China). The Cy5-labeled primers with or without the putative TCP-binding site were synthesized by TsingKe (Beijing, China). The DNA fragment was incubated with the purified protein at 25°C for 30 min, separated by 5% native PAGE (10 V/cm, 4°C) in 0.5× Tris/borate/EDTA buffer. Fluorescence was observed with an image scanner (FLA-9000; Fujifilm).

For dual-luciferase (dual-LUC) assays, promoter fragments of *GhFSN1*, *GhCESA7*, *GhEXPA1*, *GhRDL1*, and other selected genes were amplified from *G. hirsutum* cv R15 genomic DNA and ligated to the firefly luciferase (LUC) reporter gene with the primers listed (Supplemental Table 10). Coupled with a co-suppression repressor plasmid, pSoup-P19 plasmids harboring the promoter were transferred into *A. tumefaciens* cells, which were infiltrated into *N. benthamiana* leaves. Three days later the treated areas were harvested for extraction of total proteins. The Dual-Luciferase Reporter Assay System kit (E1910, Promega) was used to detect the fluorescence from LUC and Renilla (REN) luciferase with Promega GloMax 20/20. The value of LUC was normalized to that of REN.

For coIP, GhTCP4A was fused with the FLAG tag and GhHOX3 with the GFP tag. Tobacco leaves were infiltrated as described above, and the leaf proteins were extracted using an extraction buffer (pH 7.5) containing 100 mM Tris–HCl, 5 mM EDTA, 100 mM NaCl, 0.2% Nonidet P-40, 1.0% Triton-X-100, 1 mM dithiothreitol, 1 mM phenylmethylsulfonyl fluoride, 100 mM MG-132 (Sigma-Aldrich), and protease inhibitor cocktail (Roche). Immunoprecipitation was performed with Anti-GFP mAb-Magnetic Beads (MBL, D153-11). Lysates were incubated with the prewashed beads for 1 h at 4°C. The beads were then washed three times and solubilized in an appropriate volume of extraction buffer with 5× SDS loading buffer (Tiangen, Beijing, China). GhHOX3-GFP and GhTCP4-FLAG fusion proteins were detected by immunoblotting with 1:1000 diluted anti-GFP

antibody (ABclonal, AE012) and 1:1500 diluted anti-FLAG antibody (ABclonal, AE005), respectively.

The yeast two-hybrid cDNA library was constructed from *G. hirsutum* fiber RNAs, and the screening was performed as reported previously (Shan et al., 2014). For protein binding assays, ORFs of *GhHOX3*, *GhTCP4* and their truncated versions, or other CIN-type *GhTCP* genes were cloned into pGADT7 or pGBKT7. The truncations of GhTCP4 and GhHOX3 are shown in Figure 1B. In detail, the C-terminal (1–120 aa) or N-terminal (300–406 aa) fragments of GhTCP4 and the GhHOX3 fragment (153–714 aa) were amplified for plasmid construction. The homeodomain of GhHOX3 is located at 28–84 aa, the LZ domain is at 89–152 aa, and the START domain is at 226–449 aa. Assays were performed as described by Shan et al. (2014).

For BiFC, ORFs of *GhHOX3* and *GhTCP4A* or their truncated versions were fused to the LUC reporter as specifically indicated, then cloned into the JW771 and JW772 vectors (Shan et al., 2014), followed by infiltration into *N. benthamiana* leaves, which were examined by a CCD camera 3 days later. ITC assays were performed on a PEAQ-ITC (Malvern Panalytical). GhTCP4A protein (35 μM) was added to the cell, into which the double-stranded DNA solution (700 μM) was dropped in with the syringe. The temperature was set to 25°C, the reference power was 10 μcal/s, and the stir speed was 750 rpm. In total, 19 drops were set, with the first drop 0.4 μl in volume and the remainder 2 μl each. The duration of each injection was 4 s with 150-s spacing. The data were analyzed following the manufacturer's instructions.

ACCESSION NUMBERS

The authors declare that all data supporting the findings of this study are available within the article and its Supplemental Information files or are available from the corresponding author upon request. The raw sequencing data were deposited in the GSA (accession number: CRA002639) and the NCBI (accession number: PRJNA631328).

SUPPLEMENTAL INFORMATION

Supplemental Information is available at *Molecular Plant Online*.

FUNDING

This work was supported by the National Natural Science Foundation of China (31690092, 31788103, 31571251), the National Key R&D Program of China (2016YFD0100500), and the Ministry of Agriculture of China (2016ZX08010002, 2016ZX08005003).

AUTHOR CONTRIBUTIONS

J.-F.C., B.Z., T.-Z.Z., J.F.W., X.-Y.G., and X.-Y.C. conceived the research; J.-F.C., B.Z., C.-C.H., and H.-R.L. performed the experiments; J.-F.C., B.Z., C.-C.H., Z.-W.C., G.-J.H, T.Z., X.-X.S., C.-M.S., L.-J.W., and T.-Z.Z. contributed materials and/or analyzed data; X.-Y.C., J.-F.C., J.F.W., and X.-Y.G. wrote the article.

ACKNOWLEDGMENTS

We thank X.-Y. Gao, J.-Q. Li, and Z.-P. Zhang for TEM and SEM, and P. Zhang and Y.N. Fu (Shanghai Synchrotron) for assistance. No conflict of interest declared.

Received: November 18, 2019
Revised: May 3, 2020
Accepted: May 12, 2020
Published: May 15, 2020

REFERENCES

Addo-Quaye, C., Miller, W., and Axtell, M.J. (2009). CleaveLand: a pipeline for using degradome data to find cleaved small RNA targets. Bioinformatics **25**:130–131.

Altschul, S.F., Madden, T.L., Schaffer, A.A., Zhang, J., Zhang, Z., Miller, W., and Lipman, D.J. (1997). Gapped BLAST and PSI-BLAST: a new generation of protein database search programs. Nucleic Acids Res. **25**:3389–3402.

Applequist, W.L., Cronn, R., and Wendel, J.F. (2001). Comparative development of fiber in wild and cultivated cotton. Evol. Dev. **3**:3–17.

Bashline, L., Li, S.D., and Gu, Y. (2014). The trafficking of the cellulose synthase complex in higher plants. Ann. Bot. **114**:1059–1067.

Bent, A. (2006). *Arabidopsis thaliana* floral dip transformation method. In Agrobacterium Protocols, K. Wang, ed. (Totowa (NJ): Humana Press), pp. 87–104.

Challa, K.R., Aggarwal, P., and Nath, U. (2016). Activation of YUCCA5 by the transcription factor TCP4 integrates developmental and environmental signals to promote hypocotyl elongation in *Arabidopsis*. Plant Cell **28**:2117–2130.

Chen, Z.J., Sreedasyam, A., Ando, A., Song, Q., De Santiago, L.M., Hulse-Kemp, A.M., Ding, M., Ye, W., Kirkbride, R.C., Jenkins, J., et al. (2020). Genomic diversifications of five Gossypium allopolyploid species and their impact on cotton improvement. Nat. Genet. **52**:525–533.

Cosgrove, D.J. (2005). Growth of the plant cell wall. Nat. Rev. Mol. Cell Biol. **6**:850–861.

Dai, Y., Yang, J., Hu, W., Zahoor, R., Chen, B., Zhao, W., Meng, Y., and Zhou, Z. (2017). Simulative global warming negatively affects cotton fiber length through shortening fiber rapid elongation duration. Sci. Rep. **7**:9264.

Danisman, S., van der Wal, F., Dhondt, S., Waites, R., de Folter, S., Bimbo, A., van Dijk, A.D., Muino, J.M., Cutri, L., Dornelas, M.C., et al. (2012). *Arabidopsis* class I and class II TCP transcription factors regulate jasmonic acid metabolism and leaf development antagonistically. Plant Physiol. **159**:1511–1523.

Diao, Y., Zhan, J., Zhao, Y., Liu, L., Liu, P., Wei, X., Ding, Y., Sajjad, M., Hu, W., Wang, P., et al. (2019). GhTIE1 regulates branching through modulating the transcriptional activity of TCPs in cotton and *Arabidopsis*. Front. Plant Sci. **10**:1348.

Du, X., Huang, G., He, S., Yang, Z., Sun, G., Ma, X., Li, N., Zhang, X., Sun, J., Liu, M., et al. (2018). Resequencing of 243 diploid cotton accessions based on an updated A genome identifies the genetic basis of key agronomic traits. Nat. Genet. **50**:796–802.

Efroni, I., Blum, E., Goldshmidt, A., and Eshed, Y. (2008). A protracted and dynamic maturation schedule underlies *Arabidopsis* leaf development. Plant Cell **20**:2293–2306.

Fang, L., Wang, Q., Hu, Y., Jia, Y., Chen, J., Liu, B., Zhang, Z., Guan, X., Chen, S., Zhou, B., et al. (2017). Genomic analyses in cotton identify signatures of selection and loci associated with fiber quality and yield traits. Nat. Genet. **49**:1089–1098.

Foster, C.E., Martin, T.M., and Pauly, M. (2010). Comprehensive compositional analysis of plant cell walls (lignocellulosic biomass) part II: carbohydrates. J. Vis. Exp. https://doi.org/10.3791/1837.

González-Grandío, E., and Cubas, P. (2016). TCP transcription factors: evolution, structure, and biochemical function. In Plant Transcription Factors: Evolutionary, Structural and Functional Aspects, D.H. Gonzalez, ed. (Cambridge, MA: Academic Press), pp. 139–151.

Gou, J.Y., Wang, L.J., Chen, S.P., Hu, W.L., and Chen, X.Y. (2007). Gene expression and metabolite profiles of cotton fiber during cell elongation and secondary cell wall synthesis. Cell Res. **17**:422–434.

Guan, X., Song, Q., and Chen, Z.J. (2014). Polyploidy and small RNA regulation of cotton fiber development. Trends Plant Sci. **19**:516–528.

Han, L.B., Li, Y.B., Wang, H.Y., Wu, X.M., Li, C.L., Luo, M., Wu, S.J., Kong, Z.S., Pei, Y., Jiao, G.L., et al. (2013). The dual functions of

WLIM1a in cell elongation and secondary wall formation in developing cotton fibers. Plant Cell **25**:4421–4438.

Hao, J., Tu, L., Hu, H., Tan, J., Deng, F., Tang, W., Nie, Y., and Zhang, X. (2012). GbTCP, a cotton TCP transcription factor, confers fibre elongation and root hair development by a complex regulating system. J. Exp. Bot. **63**:6267–6281.

Hernandez-Gomez, M.C., Runavot, J.L., Guo, X., Bourot, S., Benians, T.A., Willats, W.G., Meulewaeter, F., and Knox, J.P. (2015). Heteromannan and heteroxylan cell wall polysaccharides display different dynamics during the elongation and secondary cell wall deposition phases of cotton fiber cell development. Plant Cell Physiol. **56**:1786–1797.

Hu, H., He, X., Tu, L., Zhu, L., Zhu, S., Ge, Z., and Zhang, X. (2016). GhJAZ2 negatively regulates cotton fiber initiation by interacting with the R2R3-MYB transcription factor GhMYB25-like. Plant J. **88**:921–935.

Hu, Y., Chen, J., Fang, L., Zhang, Z., Ma, W., Niu, Y., Ju, L., Deng, J., Zhao, T., Lian, J., et al. (2019). *Gossypium barbadense* and *Gossypium hirsutum* genomes provide insights into the origin and evolution of allotetraploid cotton. Nat. Genet. **51**:739–748.

Huang, D., Wang, S., Zhang, B., Shang-Guan, K., Shi, Y., Zhang, D., Liu, X., Wu, K., Xu, Z., Fu, X., et al. (2015). A gibberellin-mediated DELLA-NAC signaling cascade regulates cellulose synthesis in rice. Plant Cell **27**:1681–1696.

Huang, J., Chen, F., Wu, S., Li, J., and Xu, W. (2016). Cotton GhMYB7 is predominantly expressed in developing fibers and regulates secondary cell wall biosynthesis in transgenic *Arabidopsis*. Sci. China Life Sci. **59**:194–205.

Huang, C., Zhang, R., Gui, J., Zhong, Y., and Li, L. (2018). The receptor-like kinase AtVRLK1 regulates secondary cell wall thickening. Plant Physiol. **177**:671–683.

Huang, G., Wu, Z., Percy, R.G., Bai, M., Li, Y., Frelichowski, J.E., Hu, J., Wang, K., Yu, J.Z., and Zhu, Y. (2020). Genome sequence of *Gossypium herbaceum* and genome updates of *Gossypium arboreum* and *Gossypium hirsutum* provide insights into cotton A-genome evolution. Nat. Genet. **52**:516–524.

Kang, X., Kirui, A., Dickwella Widanage, M.C., Mentink-Vigier, F., Cosgrove, D.J., and Wang, T. (2019). Lignin-polysaccharide interactions in plant secondary cell walls revealed by solid-state NMR. Nat. Commun. **10**:347.

Kim, H.J., and Triplett, B.A. (2001). Cotton fiber growth in planta and in vitro. Models for plant cell elongation and cell wall biogenesis. Plant Physiol. **127**:1361–1366.

Kosugi, S., and Ohashi, Y. (1997). PCF1 and PCF2 specifically bind to cis elements in the rice proliferating cell nuclear antigen gene. Plant Cell **9**:1607–1619.

Kosugi, S., and Ohashi, Y. (2002). DNA binding and dimerization specificity and potential targets for the TCP protein family. Plant J. **30**:337–348.

Lacape, J.M., Llewellyn, D., Jacobs, J., Arioli, T., Becker, D., Calhoun, S., Al-Ghazi, Y., Liu, S., Palai, O., Georges, S., et al. (2010). Meta-analysis of cotton fiber quality QTLs across diverse environments in a *Gossypium hirsutum* x *G. barbadense* RIL population. BMC Plant Biol. **10**:132.

Lee, J.J., Woodward, A.W., and Chen, Z.J. (2007). Gene expression changes and early events in cotton fibre development. Ann. Bot. **100**:1391–1401.

Ma, Z., He, S., Wang, X., Sun, J., Zhang, Y., Zhang, G., Wu, L., Li, Z., Liu, Z., Sun, G., et al. (2018). Resequencing a core collection of upland cotton identifies genomic variation and loci influencing fiber quality and yield. Nat. Genet. **50**:803–813.

Mansoor, S., and Paterson, A.H. (2012). Genomes for jeans: cotton genomics for engineering superior fiber. Trends Biotechnol. **30**:521–527.

McFarlane, H.E., Doring, A., and Persson, S. (2014). The cell biology of cellulose synthesis. Annu. Rev. Plant Biol. **65**:69–94.

Nath, U., Crawford, B.C.W., Carpenter, R., and Coen, E. (2003). Genetic control of surface curvature. Science **299**:1404–1407.

Palatnik, J.F., Allen, E., Wu, X.L., Schommer, C., Schwab, R., Carrington, J.C., and Weigel, D. (2003). Control of leaf morphogenesis by microRNAs. Nature **425**:257–263.

Paterson, A.H., Wendel, J.F., Gundlach, H., Guo, H., Jenkins, J., Jin, D.C., Llewellyn, D., Showmaker, K.C., Shu, S.Q., Udall, J., et al. (2012). Repeated polyploidization of *Gossypium* genomes and the evolution of spinnable cotton fibres. Nature **492**:423.

Pettolino, F.A., Walsh, C., Fincher, G.B., and Bacic, A. (2012). Determining the polysaccharide composition of plant cell walls. Nat. Protoc. **7**:1590–1607.

Qin, Y.M., and Zhu, Y.X. (2011). How cotton fibers elongate: a tale of linear cell-growth mode. Curr. Opin. Plant Biol. **14**:106–111.

Qin, Y.M., Hu, C.Y., Pang, Y., Kastaniotis, A.J., Hiltunen, J.K., and Zhu, Y.X. (2007). Saturated very-long-chain fatty acids promote cotton fiber and *Arabidopsis* cell elongation by activating ethylene biosynthesis. Plant Cell **19**:3692–3704.

Rombola-Caldentey, B., Rueda-Romero, P., Iglesias-Fernandez, R., Carbonero, P., and Onate-Sanchez, L. (2014). *Arabidopsis* DELLA and two HD-ZIP transcription factors regulate GA signaling in the epidermis through the L1 box cis-element. Plant Cell **26**:2905–2919.

Ruan, Y.L., Llewellyn, D.J., and Furbank, R.T. (2001). The control of single-celled cotton fiber elongation by developmentally reversible gating of plasmodesmata and coordinated expression of sucrose and K^+ transporters and expansin. Plant Cell **13**:47–60.

Schommer, C., Palatnik, J.F., Aggarwal, P., Chetelat, A., Cubas, P., Farmer, E.E., Nath, U., and Weigel, D. (2008). Control of jasmonate biosynthesis and senescence by miR319 targets. PLoS Biol. **6**:e230.

Shan, C.-M., Shangguan, X.-X., Zhao, B., Zhang, X.-F., Chao, L.-M., Yang, C.-Q., Wang, L.-J., Zhu, H.-Y., Zeng, Y.-D., Guo, W.-Z., et al. (2014). Control of cotton fibre elongation by a homeodomain transcription factor GhHOX3. Nat. Commun. **5**:5519.

Shangguan, X.X., Xu, B., Yu, Z.X., Wang, L.J., and Chen, X.Y. (2008). Promoter of a cotton fibre MYB gene functional in trichomes of *Arabidopsis* and glandular trichomes of tobacco. J. Exp. Bot. **59**:3533–3542.

Song, D., Sun, J., and Li, L. (2014). Diverse roles of PtrDUF579 proteins in Populus and PtrDUF579-1 function in vascular cambium proliferation during secondary growth. Plant Mol. Biol. **85**:601–612.

Sun, X., Gong, S.Y., Nie, X.Y., Li, Y., Li, W., Huang, G.Q., and Li, X.B. (2015). A R2R3-MYB transcription factor that is specifically expressed in cotton (*Gossypium hirsutum*) fibers affects secondary cell wall biosynthesis and deposition in transgenic *Arabidopsis*. Physiol. Plant **154**:420–432.

Sun, X., Wang, C., Xiang, N., Li, X., Yang, S., Du, J., Yang, Y., and Yang, Y. (2017). Activation of secondary cell wall biosynthesis by miR319-targeted TCP4 transcription factor. Plant Biotechnol. J. **15**:1284–1294.

Szymanski, D.B., Lloyd, A.M., and Marks, M.D. (2000). Progress in the molecular genetic analysis of trichome initiation and morphogenesis in *Arabidopsis*. Trends Plant Sci. **5**:214–219.

Takenaka, Y., Watanabe, Y., Schuetz, M., Unda, F., Hill, J.L., Jr., Phookaew, P., Yoneda, A., Mansfield, S.D., Samuels, L., Ohtani, M., et al. (2018). Patterned deposition of xylan and lignin is independent from that of the secondary wall cellulose of *Arabidopsis* xylem vessels. Plant Cell **30**:2663–2676.

Tan, J., Walford, S.A., Dennis, E.S., and Llewellyn, D. (2016). Trichomes control flower bud shape by linking together young petals. Nat. Plants **2**:16093.

Taylor-Teeples, M., Lin, L., de Lucas, M., Turco, G., Toal, T.W., Gaudinier, A., Young, N.F., Trabucco, G.M., Veling, M.T., Lamothe, R., et al. (2015). An *Arabidopsis* gene regulatory network for secondary cell wall synthesis. Nature **517**:571–575.

Tuttle, J.R., Nah, G., Duke, M.V., Alexander, D.C., Guan, X., Song, Q., Chen, Z.J., Scheffler, B.E., and Haigler, C.H. (2015). Metabolomic and transcriptomic insights into how cotton fiber transitions to secondary wall synthesis, represses lignification, and prolongs elongation. BMC Genomics **16**:477.

Vadde, B.V.L., Challa, K.R., and Nath, U. (2018). The TCP4 transcription factor regulates trichome cell differentiation by directly activating GLABROUS INFLORESCENCE STEMS in *Arabidopsis thaliana*. Plant J. **93**:259–269.

Walford, S.-A., Wu, Y., Llewellyn, D.J., and Dennis, E.S. (2011). GhMYB25-like: a key factor in early cotton fibre development. Plant J. **65**:785–797.

Wang, S., Wang, J.W., Yu, N., Li, C.H., Luo, B., Gou, J.Y., Wang, L.J., and Chen, X.Y. (2004). Control of plant trichome development by a cotton fiber MYB gene. Plant Cell **16**:2323–2334.

Wang, M.Y., Zhao, P.M., Cheng, H.Q., Han, L.B., Wu, X.M., Gao, P., Wang, H.Y., Yang, C.L., Zhong, N.Q., Zuo, J.R., et al. (2013). The cotton transcription factor TCP14 functions in auxin-mediated epidermal cell differentiation and elongation. Plant Physiol. **162**:1669–1680.

Wang, M., Tu, L., Lin, M., Lin, Z., Wang, P., Yang, Q., Ye, Z., Shen, C., Li, J., Zhang, L., et al. (2017). Asymmetric subgenome selection and cis-regulatory divergence during cotton domestication. Nat. Genet. **49**:579–587.

Wendel, J.F., and Grover, C.E. (2015). Taxonomy and evolution of the cotton genus, *Gossypium*. In Cotton, *Vol. 57*, 2nd edition, , D.D. Fang and R.G. Percy, eds. (New York: Wiley) https://doi.org/10.2134/agronmonogr57.2013.0020.

Wu, H., Tian, Y., Wan, Q., Fang, L., Guan, X., Chen, J., Hu, Y., Ye, W., Zhang, H., Guo, W., et al. (2018). Genetics and evolution of MIXTA genes regulating cotton lint fiber development. New Phytol. **217**:883–895.

Xu, B., Gou, J.Y., Li, F.G., Shangguan, X.X., Zhao, B., Yang, C.Q., Wang, L.J., Yuan, S., Liu, C.J., and Chen, X.Y. (2013). A cotton BURP domain protein interacts with alpha-expansin and their co-expression promotes plant growth and fruit production. Mol. Plant **6**:945–958.

Xu, P., Cai, X.T., Wang, Y., Xing, L., Chen, Q., and Xiang, C.B. (2014). HDG11 upregulates cell-wall-loosening protein genes to promote root elongation in *Arabidopsis*. J. Exp. Bot. **65**:4285–4295.

Yuan, D., Tang, Z., Wang, M., Gao, W., Tu, L., Jin, X., Chen, L., He, Y., Zhang, L., Zhu, L., et al. (2015). The genome sequence of Sea-Island cotton (*Gossypium barbadense*) provides insights into the allopolyploidization and development of superior spinnable fibres. Sci. Rep. **5**:17662.

Zhang, T., Hu, Y., Jiang, W., Fang, L., Guan, X., Chen, J., Zhang, J., Saski, C.A., Scheffler, B.E., Stelly, D.M., et al. (2015). Sequencing of allotetraploid cotton (*Gossypium hirsutum* L. acc. TM-1) provides a resource for fiber improvement. Nat. Biotechnol. **33**:531–537.

Zhang, Z., Ruan, Y.L., Zhou, N., Wang, F., Guan, X., Fang, L., Shang, X., Guo, W., Zhu, S., and Zhang, T. (2017). Suppressing a putative sterol carrier gene reduces plasmodesmal permeability and activates sucrose transporter genes during cotton fiber elongation. Plant Cell **29**:2027–2046.

Zhang, J., Huang, G.Q., Zou, D., Yan, J.Q., Li, Y., Hu, S., and Li, X.B. (2018). The cotton (*Gossypium hirsutum*) NAC transcription factor (FSN1) as a positive regulator participates in controlling secondary cell wall biosynthesis and modification of fibers. New Phytol. **217**:625–640.

Zhao, B., Cao, J.F., Hu, G.J., Chen, Z.W., Wang, L.Y., Shangguan, X.X., Wang, L.J., Mao, Y.B., Zhang, T.Z., Wendel, J.F., et al. (2018). Core cis-element variation confers subgenome-biased expression of a transcription factor that functions in cotton fiber elongation. New Phytol. **218**:1061–1075.